arthropoda

MDPI

Article

Evidence and Modification of Non-Visual Eyestalk Organs in Troglobiont Mysida and Stygiomysida (Crustacea)

Karl J. Wittmann

Department of Environmental Health, Medical University of Vienna, 1090 Vienna, Austria; karl.wittmann@meduniwien.ac.at

Abstract: Why do the eyes remain comparatively large, whereas the cornea is reduced in most troglobiont mysids? Are there any important organ size-dependent functions served by non-visual eye rudiments? This issue was approached by measuring eye structures in five troglobiont species of Mysida and two Stygiomysida compared with 14 troglophiles and 49 trogloxene Mysida species. The Organ of Bellonci (OB) was found in all Mysida and, as first records, also in Stygiomysida. The length of OBs increased with individual body length (BL) and eye length (EL) in four examined species: from postnauplioid larvae to adult stage in a troglophile and a trogloxene mysid species examined; and from juveniles to adults in a troglobiont mysid and a troglobiont stygiomysid. At the interspecific level, EL was, on average, 26% shorter at a given BL, while the OB was 40% longer at a given BL and 54% longer at a given EL, respectively, in adult troglobionts compared with trogloxene mysids. The OB is clearly proliferating, while the cornea is reduced in troglobionts. This points to sensory functions (possibly together with other functions). The sensory pore organ was found in all 15 Mysida species whose eyes were mounted on slides, and the first record of this organ was also found in Stygiomysida.

Keywords: troglophilia; ontogeny; eye structure; size of Organ of Bellonci; sensory pore organ

Citation: Wittmann, K.J. Evidence and Modification of Non-Visual Eyestalk Organs in Troglobiont Mysida and Stygiomysida (Crustacea). *Arthropoda* **2023**, *1*, 432–450. https://doi.org/10.3390/arthropoda1040019

Academic Editor: Charles Fransen

Received: 20 July 2023
Revised: 27 October 2023
Accepted: 7 November 2023
Published: 14 November 2023

1. Introduction

Our knowledge of non-visual eyestalk organs in mysidaceans is far from exhaustive. An Organ of Bellonci (OB) was indicated mostly without details as a circle or as an oval in drawings of eyes for an estimated fifty of the currently acknowledged 1224 species of Mysida (own census 2 July 2023). The OB is located near the base of each eyestalk and on or near a sensory papilla, if present. It was described as a bipartite vesicle connected to a proximal nerve; the completely internal OB is closely accompanied by sensory pores reaching the surface of the cuticle [1]. OBs are found in the eyestalks of most podophthalmous crustaceans, whereas sensory pore organs (SPOs) have a more restricted distribution in this crustacean group [2]. OBs and SPOs form separate organs developing independently in the shrimp *Palaemon serratus* (Pennant, 1777) [3].

To date, non-visual eyestalk organs were completely unknown in all 16 currently acknowledged species of Stygiomysida, most of which are anophthalmic, living in hypogean aquatic environments. Only three species show a few functional ommatidia distolaterally on the eyestalks: *Spelaeomysis servata* (Fage, 1924) (gender of species name here corrected due to fixation of '*Mysis*' as feminine [4] (p. 129)) from a dimly-lit dolina in Zanzibar and a tide-pool in Aldabra, W-Indian Ocean; *S. cardisomae* Bowman, 1973, from burrows of land crabs along the Caribbean coast of Columbia and from the coast of Peru, this species also occurring in caves; and *S. cochinensis* Panampunnayil & Viswakumar, 1991, from a prawn culture field fully exposed to sunlight in Cochin, India. A fourth species not fully restricted to darkness, the anophthalmic *S. bottazzii* Caroli, 1924, from the Salento Peninsula (S-Italy), inhabits deep brackish groundwater but also shallow wells and dolinas, where it exhibits microphytophagy in or near the margins of the photic zone during part of its life cycle [5,6].

With these four species occurring at least partly in photic habitats, the genus *Spelaeomysis* Caroli, 1924, appears less strongly tied to dark, deep groundwater than generally assumed up to the 1960s. Future intensified studies in 'small' habitats such as dolinas and wells could reveal additional ties of Stygiomysida species to photic habitats.

A potential chemoreceptive function of SPOs was considered to be speculative as long as it was based solely on ultrastructure [2]. Based on the structure of the OB, a sensory function—either chemosensory or photoreceptive—rather than a neurosecretory function was hypothesized as most probable. Nonetheless, this did not exclude potentially differing functions between crustacean groups [2]. In favor of this interpretation, a neurosecretory role was demonstrated mainly in the gut, where genes coding for neuropeptides were expressed, and less in the OB, optic nerve in the eyestalk or in other organs of a decapod shrimp [7].

An ultrastructural study of the OB in the amphipod *Gammarus setosus* Dementieva, 1931, led to the statement that [8] "The large size, cephalic position, elaborate structure, and suspension of the organ suggest that it is of considerable importance in the sensory capability of aquatic Malacostraca." Nonetheless, a potential sensory capability could hardly be generalized for all aquatic Malacostraca in view of recent findings pointing to the function of the OB in endocrine control [7,9]. The precise functions are unknown in Mysida and Stygiomysida. The below documented large-sized OB shared by certain mysidaceans with species of *Gammarus* Fabricius, 1775, would be strange if the OB were an exclusively endocrine organ. The first ample multi-species investigation on potential ties between habitat and qualitative and metric features of the eyestalk is presented to shed light on this issue. This could revive discussions [7–10] on potential sensory functions of non-visual eyestalk organs and provide stimuli for future research in this field.

2. Materials and Methods

2.1. Terminology and Definitions

The terminology and distinction of stages are based on previous publications [11,12] unless explicitly addressed below. 'Neonates' are freshly molted individuals from larval to juvenile stage upon release from the brood pouch. 'Mysidaceans' is used as an informal combination of the orders Mysida and Stygiomysida. The terms 'troglobiont', 'troglophile', and 'trogloxene' are increasingly being used [13]. The species are categorized as troglobiont (stygobiontic) and troglophile (stygophilic), mostly in agreement with Pesce et al. [14]. Troglobionts have the cornea strongly reduced, and at least the adults mostly inhabit caves or groundwater. Troglophile species have mostly functional eyes; nonetheless, they are sciaphilic and regularly but not exclusively found in these habitats. Trogloxene species are photo-sensory competent and are not or rarely found in these habitats. As an exception from the categorization by Pesce et al., *Leptomysis buergii* Băcescu, 1966, is here categorized as trogloxene rather than troglophile because it forms hyperbenthic swarms mostly above sandy bottoms and only exceptionally inhabits caves [15]. Additional species not treated by Pesce et al., namely *Diamysis camassai* Ariani & Wittmann, 2002; *Heteromysis ekamako* Wittmann & Chevaldonné, 2016; *Mysidetes hanseni* Zimmer, 1914, and *M. illigi* Zimmer, 1914, are here categorized as troglophile based on recent records from hypogean aquatic environments [5,12,16]. Finally, *Siriella gracilipes* H. Nouvel, 1942, is categorized as a troglophile due to its well-known massive presence in intertidal marine caves of the Mediterranean during daytime. All other species listed in Table S1 are trogloxene

2.2. Materials

Sampling data are available in Table S1 along with BL, EL, OBL (abbreviations in Section 2.4), and the qualitative variable TR for 68 species of Mysidae (Mysida). This encompasses 5 troglobiont, 14 troglophiles, and 49 trogloxene species, together with two species of troglobiont Stygiomysida. Studies at the interspecific level are based on 1–5 specimens per mysid species, yielding a total of 286 specimens (280 adults and 6 subadults); the stygiomysids are represented by 24 adult *Spelaeomysis bottazzii* and one subadult *Sty-*

giomysis major Bowman, 1976. Additional samples were used to study three mysid and one stygiomysid species at the intraspecific level, covering larvae and juveniles to adults; these specimens are represented individually by data points in Figures 4 and 9. Six postnauplioid larvae and three neonates from a published [6,17] former laboratory culture of *S. bottazzii* originating from a brackish well (Table S1) in southern Italy are included.

Most materials were collected from 1974 to 2015 by the present author during sampling campaigns in marine and continental waters of the W and E-Atlantic, Mediterranean, Black Sea, and Red Sea Basins and by Antonio P. Ariani (Naples) during research trips to Mediterranean waters from 1965 to 2011. Extensive materials were gained by the exchange of collection materials with Torleiv Brattegard (Bergen), Masaaki Murano (Tokyo), and W. Wayne Price (Tampa); and with the meanwhile deceased Mihai Băcescu (1908–1999) (Bucharest), Thomas E. Bowman (1934–2013) (Washington), Victor V. Petryashov (1956−2018) (St. Petersburg), and Boris Šket (1936–2023) (Ljubljana). Additional important contributions were made by academic and citizen scientists listed in the acknowledgments below. Further materials were studied upon visits and based on loans, respectively, from museum collections in Bucharest, Frankfurt am Main, Munich, and Vienna and from collections of the Fisheries Institute (INPA) of Manaus, Brazil. Due to the heterogenic sources, the available materials showed great differences in the mode of fixation and state of preservation.

2.3. Methods

Measurements, preparation, and microscopy are as previously published [12]. BL (mm) was measured from the tip of the rostrum to the terminal margin of the telson in free-living stages or as an unspecific anteroposterior extension in marsupial larvae with the rostrum and telson not yet fully differentiated. EL (mm) measured along the midline from the insertion at frons to the distalmost point, including, if any, the cornea. OBL (µm) is the length of the mostly ellipsoidal, ovoid, or pyriform organ and has a diameter in the case of a spherical organ (bipartite organs treated as if fused). Entire specimens in 80% ethanol were studied using the binocular microscope Nikon SMZ-U, and objects mounted on slides in Swan (=Swann) medium using a Nikon Eclipse 80i, in each case with photo cameras giving a frame of 2880 × 2048 pixels. The camera data were integrated by the program NIS-Elements D 5.21.00 64-bit. The resulting images showed a green or blue tint in colorless (bleached) and white objects, giving superior distinctiveness compared with grey halftone images.

T-tests for differences between regression slopes were performed 'manually' [18]. All other tests were made with the program XLSTAT [19]. The length of the body, eyes, and OB (Figures 5 and 6) were collinear among each other. This required some data transformation to extract the potential quantitative effects of TR on these variables. As the first step, linear regressions between pairs of variables were calculated based on data from paired categories of TR (f.i. troglobiont versus trogloxene). ANOVA was then used to estimate the differences between the two cohorts of regression residuals (=distances from the regression line) obtained for the respective TRs. In favor of readability, the resulting means and confidence intervals in Table 1 were transformed post hoc to percentages. The mean of the dependent variable in the category with the most specimens was chosen as the denominator when calculating percentages.

2.4. Abbreviations

BL = body length (mm)
DD = decimal degrees of geographic coordinates
EL = eye length (mm) measured along the midline
N1–N3 = nauplioid larvae at substages N1 to N3
OB = Organ of Bellonci
OBL = length (µm) of OB
psu = practical salinity unit
SPO = sensory pore organ

TR = troglophilia with 'level' increasing from the trogloxene to troglophile and troglobiont categories

3. Results

3.1. Eye Structure in Mysida

3.1.1. Structure of Adult Eyes

Eye rudiments of free-living stages of *Troglomysis vjetrenicensis* Stammer, 1933, from freshwaters of the Vjetrenica Cave (coordinates in Table S1) are roughly V to U-shaped and project about 30–50% beyond the short, rounded rostral projection of the carapace (Figure 1B). Eyes distally with roughly spherical to oviform bodies are here interpreted as strongly rudimentary ommatidia (Figure 1C). Eye rudiments with optically dense mesial bulges are labeled '*mb*' in Figure 1B. Inspection of mounted bulges (Figure 1D) revealed an entirely internal accumulation of cells and inclusions as in the OB of the here-examined *D. lacustris* Băcescu, 1940 (Figure 2B). As in most mysids [20,21], the OBs of *T. vjetrenicensis* and *D. lacustris* form a cell complex immediately below the dorsal cuticle near the base of the eyestalk [1,22]. The OBs of both species are also characterized by two subunits (Figure 2B) containing several onion-like bodies and sensory cells with a neck ('*sc*' in Figure 1D). A field of pores (Figure 1E) interpreted as belonging to the SPO [2] was detected on the dorsal face above the OB in *T. vjetrenicensis*.

Circular to oval shallow depressions similar to those in decapods [2], here also interpreted as SPOs, were found dorsally near the OB of eyes mounted on slides in *D. lacustris* and *D. lagunaris* Ariani & Wittmann, 2000 (Figure 2C,D) and in twelve other mysid species. A depression with a central pore surrounded by a toroid was located at the tip of the sensory papilla on the eyestalk of *M. gibbosa* G.O. Sars, 1864 (Figure 2E,F), in this case, distant from the OB. Depending on fixation and on the 'expansion' of chromatophores, pale pigment-free, roughly oval spots ('*fe*' in Figure 2C) were found on the dorsal face of the eyestalk near the OB and close to the cornea in *D. lacustris* and *D. lagunaris*. These spots, termed '*fenestrae*' [22], clearly favor light penetration to the ganglion mass inside the eyestalk.

3.1.2. Size and Structure of Larval Eyes

In *T. vjetrenicensis*, all the available incubating females carried nauplioid larvae, sampled independently by A.P. Ariani and B. Šket in September of various years. Eight females with BL 10.2–13.1 mm carried 8–12 nauplioid larvae at substage N2. The BL of nauplioids ranged within 1.57–2.25 mm (n = 30). The number of larvae per female significantly increased (t-statistics, n = 8, r = 0.81, $p < 0.02$), while larval size decreased with parental size (n = 30, r = −0.41, $p < 0.03$). The maximum anteroposterior extension of the larval eyes was 0.17–0.35 mm or 10–17% BL, respectively. Eye size was significantly correlated with body size (r = 0.68, $p < 0.01$), whereas eye size expressed as a percentage of body size was not correlated (r = 0.01, $p < 0.96$). The eye proportions of N2-larvae are very similar to those of related species even though eye diameters at a given body size are mostly about 1/3 smaller, for example compared with larvae (Figure 3D versus Figure 3B) of *D. fluviatilis* Wittmann & Ariani, 2012, from the Sile River, a tributary of the N-Adriatic Sea; the latter species has large, fully functional eyes in free-living stages.

As early as at substage N2, the nauplioids of *T. vjetrenicensis* show features typical of the reduced eyes in adults: a demarcated distal area (labeled '*cr*' in Figure 3C) with a position corresponding to the corneal rudiment ('*cr*' in Figure 1C) in adults; another demarcated mid-mesial area ('*mb*' in Figure 3C) otherwise containing the OB (Figure 1D) in free-living stages. No Obs were detected in the nauplioid larvae of any mysid species. By contrast, OBs were found in the more advanced eyes of postnauplioid larvae in *D. fluviatilis*, *D. lagunaris*, and *H. microps* (G.O. Sars, 1877) (Figure 3E,F). Postnauplioids of *T. vjetrenicensis* were not available for study.

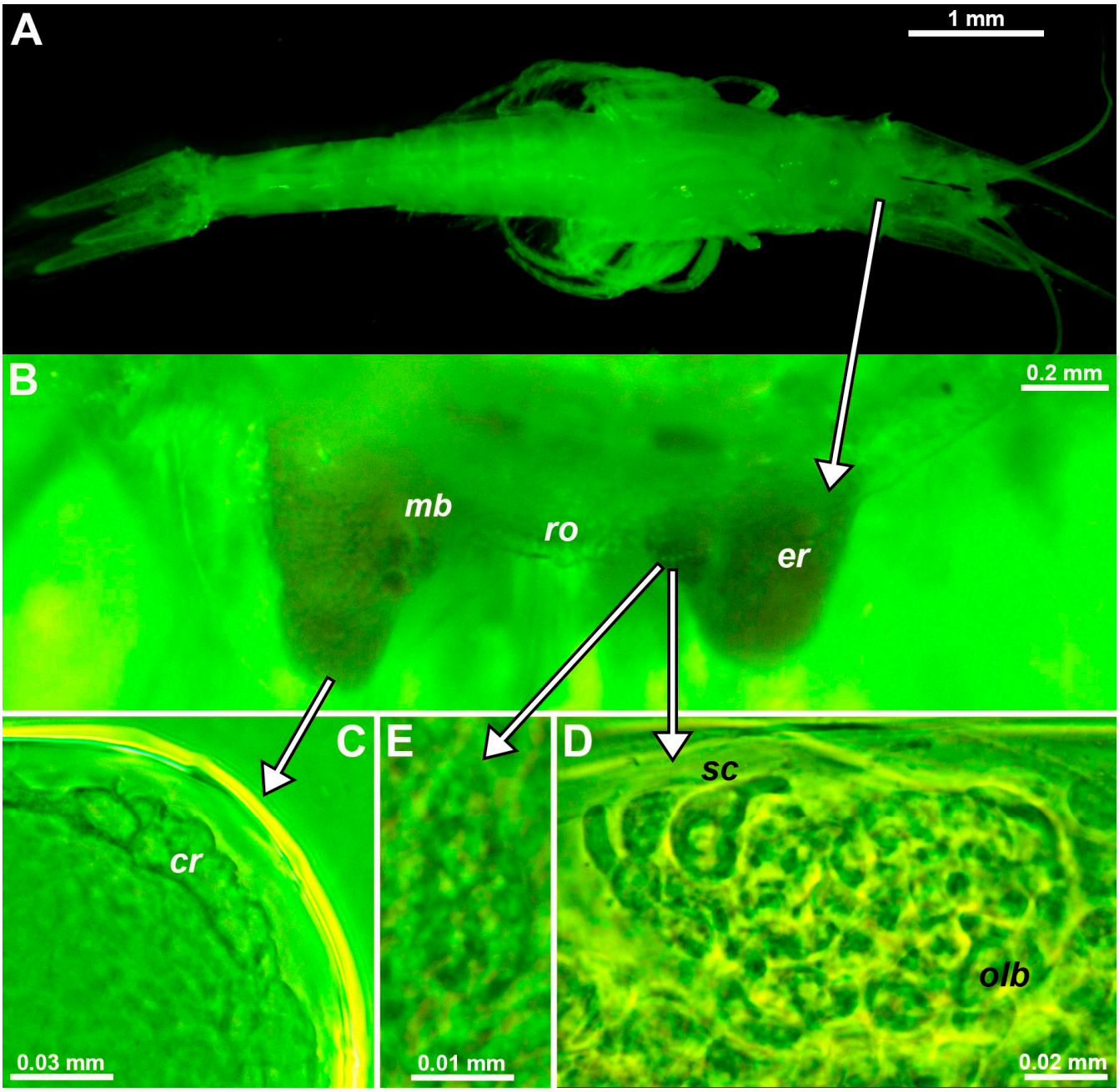

Figure 1. Eye structure in the troglobiont *Troglomysis vjetrenicensis*. (**A**) Habitus of an adult male, dorsal. (**B**) Anterior margin of the carapace and eye rudiments in upside-down orientation, dorsal, details from other specimens showing corneal rudiment (**C**) at the distal margin of the eye, OB (**D**) close to the mesial margin and pore field (**E**) at the dorsal face above the OB. Lowercase labels indicate corneal rudiment (*cr*), eye rudiment (*er*), onion-like bodies (*olb*), rostrum (*ro*), and sensory cells (*sc*). (**C**–**E**), objects expanded on the slide. The green coloring of objects is artificial.

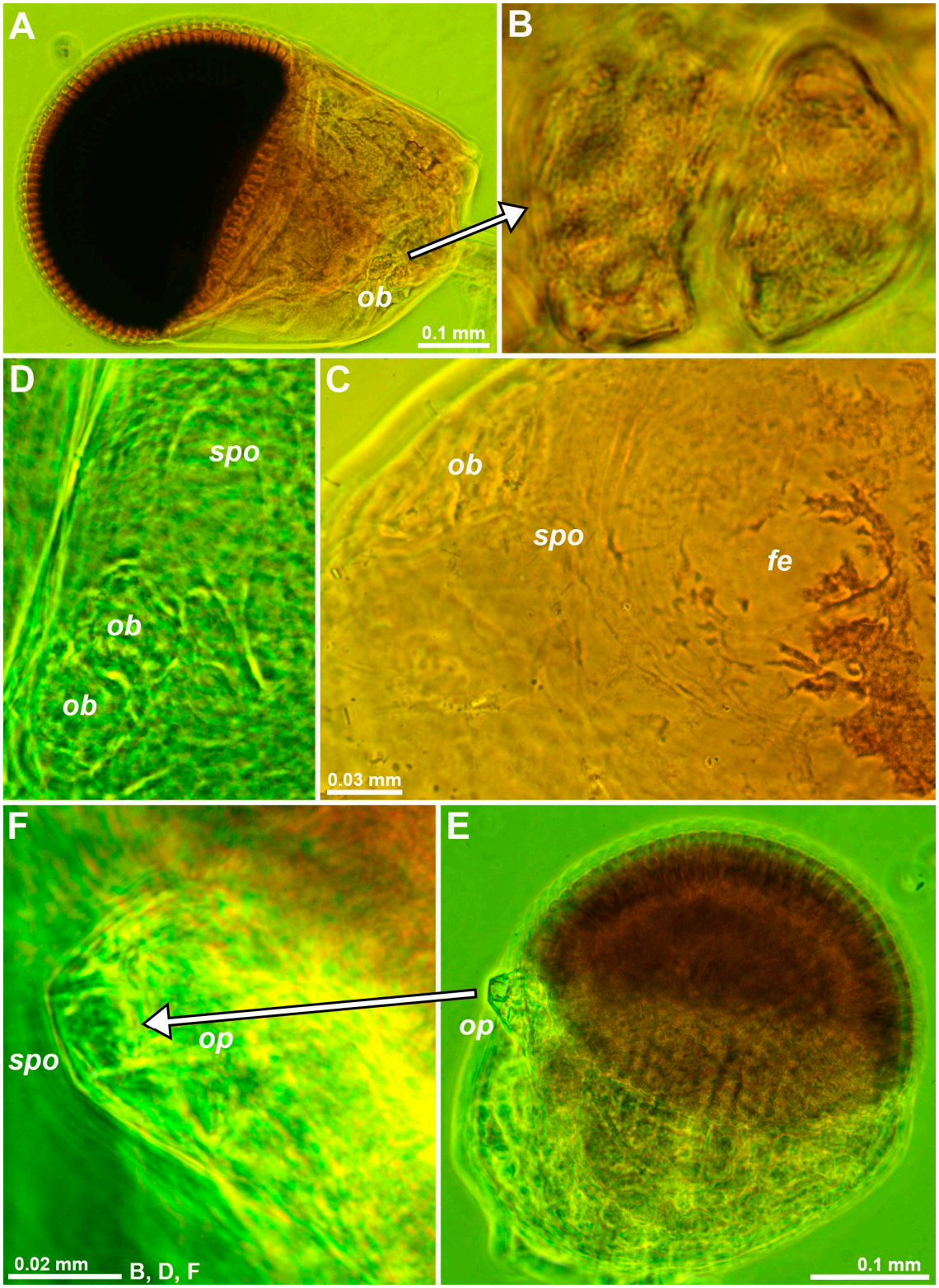

Figure 2. Structure of eyestalks in the trogloxenes *Diamysis fluviatilis* (**A**,**B**), *D. lagunaris* (**C**,**D**), and *Mysidopsis gibbosa* (**E**,**F**). (**A**) Left eye, dorsal, detail (**B**) showing a vesicular form of the OB. (**C**) Antero-mesial area of eyestalk, dorsal, focus on a '*fenestra*'. (**D**) OB and SPO in another specimen. (**E**) Left eye, dorsal, detail (**F**) showing the tip of the ocular papilla with SPO. Lowercase labels indicate *fenestra* (*fe*), OB (*ob*), ocular papilla (*op*), and SPO (*spo*). Objects expanded on the slide. The green coloring of objects is artificial.

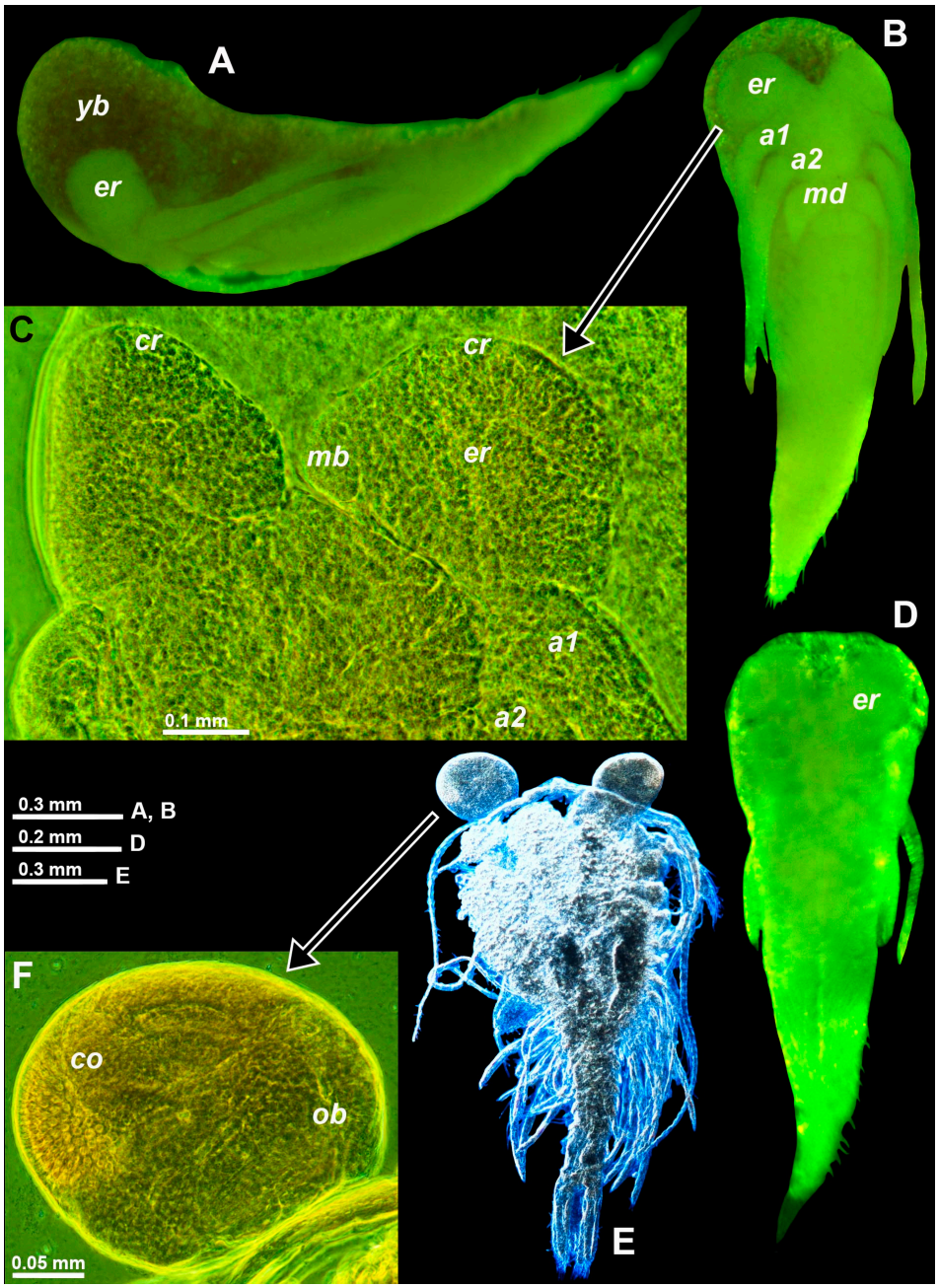

Figure 3. Eye development of marsupial larvae in the troglobiont *Troglomysis vjetrenicensis* from the cave Donja Vjetrenica (**A**–**C**), in the trogloxene *Diamysis fluviatilis* from the Sile River (**D**) and *Heteromysis microps* from the marine sublittoral in Sardinia (**E**,**F**). (**A**,**B**,**D**) Nauplioids in toto, lateral (**A**), and ventral (**B**,**D**). (**C**) The cephalic region of the nauplioid expanded on the slide, ventral. (**E**) The postnauplioid larva expanded on the slide, dorsal, detail (**F**) showing the left eye. Lowercase labels indicate antennula (*a1*), antenna (*a2*), cornea (*co*), corneal rudiment (*cr*), eye rudiment (*er*), mesial bulge (*mb*), mandible (*md*), OB (*ob*), and yolk or fat bodies (*yb*). (**A**,**B**,**D**,**E**), objects artificially separated from the background. The green and blue coloring of objects is artificial.

3.1.3. Size of the Organ of Bellonci at Intraspecific Level

The OBL versus EL and BL was measured in postnauplioid larvae and free-living stages of *D. lagunaris* (trogloxene) and *Hemimysis speluncola* Ledoyer, 1963 (troglophile); this was measured only in the free-living stages of *T. vjetrenicensis* (troglobiont) because no postnauplioids were available in this species. BL was a significant predictor of OBL in

the free-living stages of *H. speluncola* and *D. lagunaris* but not in *T. vjetrenicensis* (1, 28 d.f.; F = 0.19; $p = 0.66$).

By contrast, the data yielded significant ($p < 0.002$) linear regressions with EL as a predictor variable and OBL as a response variable in the free-living stages of every species (Figure 4). The slopes of these regressions were not significantly different from each other (t < 0.34; $p > 0.5$; $n = 54, 47, 30$, respectively). Thus, the OBLs at a given EL were calculated as mean OBLs plus residuals from the regressions given above, resulting in the mean ± s.d. being 53.78 ± 10.66 µm ($n = 54$) for *D. lagunaris*, 71.94 ± 11.93 µm ($n = 47$) for *H. speluncola*, and 96.27 ± 16.76 µm ($n = 30$) for *T. vjetrenicensis*. The non-parametric Kruskal–Wallis test was used due to samples of unequal size from different sources (species). The differences between the three species sampled were highly significant (2 d.f., K = 81.5, $p < 0.0001$). In other words, when comparing these three species, the OBL increased with increasing levels of troglophilia at a given eye size.

Figure 4A shows that the postnauplioids of *D. lagunaris* fitted the regression line of the free-living stages well. By contrast, the OBLs of all eleven available postnauplioids in *H. speluncola* (Figure 4B) were significantly below the regression line for the free-living stages (mean distance ± s.d.: −11.73 ± 5.72 µm; t = −6.8, $p < 0.0001$).

3.1.4. Size of the Organ of Bellonci at Interspecific Level

The OB was found in the eyestalks of 68 mysid species studied (individual data in Table S1), covering the subfamilies Siriellinae, Mysinae, Leptomysinae, Palaumysinae and Heteromysinae. Five other subfamilies are not represented because they lack troglobiont and troglophile species. The variables BL, EL, and OBL were significantly positively correlated with each other (Pearson $p < 0.0001$; $n = 286$).

ANCOVA yielded a significant model with BL and TR as predictors of EL (F-test; 3, 282 d.f.; F = 653.8; $p < 0.0001$). All considered parameters were highly significant ($p < 0.0001$); namely, EL strongly increased with BL (t-Test; t = 43.2) and decreased between the troglobiont and troglophile levels of TR (t = −4.4), the troglobiont level differing from the trogloxene level again stronger (t = −7.3). This model illustrates the significant reduction of eye size with increasing levels of TR. Based on this model, a linear regression analysis with BL as a predictor variable and EL as a response variable was performed separately for the trogloxene, troglophile, and troglobiont mysid species. The individual data and resulting regression lines, the latter with a $p < 0.0001$, are visualized in Figure 5. Effects of TR on EL at a given BL were estimated using ANOVA on the regression residuals versus paired TRs as outlined in the 'Materials and Methods'; for the results, see Table 1.

A first run of ANCOVA with BL, EL, and TR as predictors of OBL also yielded a significant model. However, the components BL (t = 2.0; $p = 0.053$) and the difference between the troglophile and trogloxene TRs (t = 0.2; $p = 0.87$) were insignificant. The lack of significance in BL is attributed to high collinearity with EL (r = 0.92; $n = 286$; $p < 0.0001$). Eliminating insignificant and collinear predictors yielded a significant model (2, 283 d.f.; F = 167.9; $p < 0.0001$), constituted by EL (t = 17.5; $p < 0.0001$) and troglobiont versus combined troglophile and trogloxene TRs (t = 9.0; $p < 0.0001$) as significant predictors of OBL. Based on this model, a linear regression analysis with EL as a predictor variable and OBL as a response variable was performed separately for troglobiont and for the combined troglophile and trogloxene TRs. The individual data and resulting regression lines are shown in Figure 6. Effects of TR on OBL at a given EL and in separate computations at a given BL were estimated as in Section 2.3, results given in Table 1.

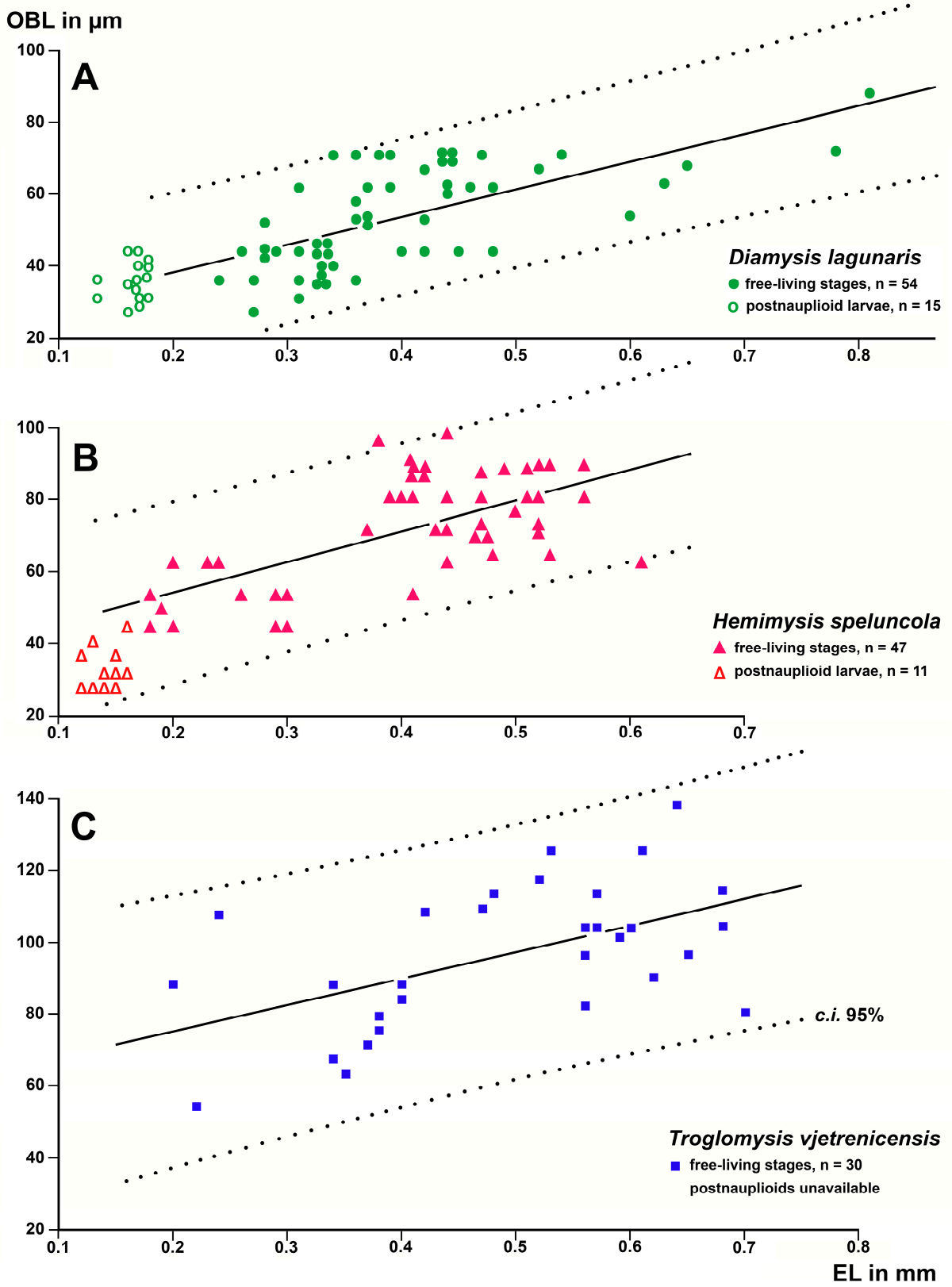

Figure 4. Length of the OBL as a response variable with EL as a predictor variable in linear regressions of larval and free-living specimens of trogloxene (**A**), troglophile (**B**), and troglobiont (**C**) mysid species. Regressions were calculated with data from free-living specimens only; data points for postnauplioid larvae were added post hoc. Coinciding points are slightly displaced.

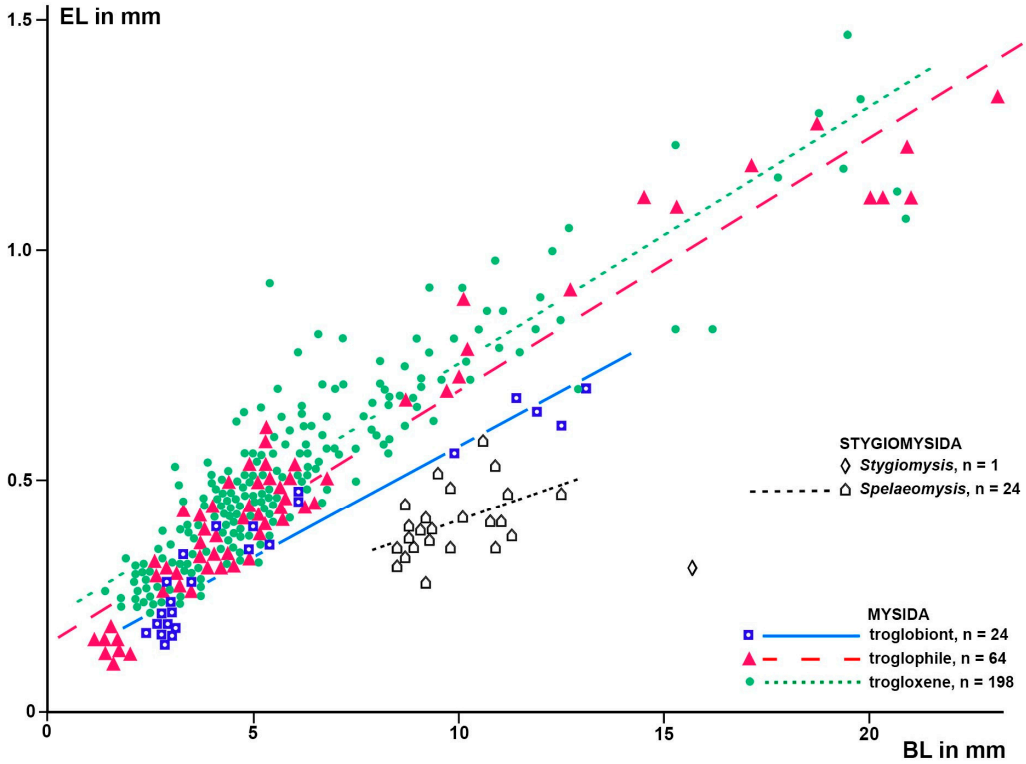

Figure 5. EL as a response variable versus BL as a predictor variable in separate linear regressions for the stygiomysid *Spelaeomysis bottazzii* (24 adult specimens) and for the troglobiont, troglophile, and trogloxene mysids (286 specimens of 68 species). Coinciding points are slightly displaced.

Table 1. Effects of troglophilia on length of eyes (mm) and Organ of Bellonci (μm) in mysidaceans.

		Troglobiont vs. Troglophile Mysida	**Troglobiont vs. Trogloxene Mysida**	**Troglophile vs. Trogloxene Mysida**	**Troglobiont Mysida vs. Stygiomysida**
	n species n specimens	5 + 14 24 + 64	5 + 49 24 + 198	14 + 49 64 + 198	5 + 2 24 + 25
Effects on EL at given BL	mean ± s.e. c.i. 95% P (2-tailed) % mean (c.i.)	−0.086 ± 0.019 −0.123 to −0.049 <0.0001 −17% (76–90%)	−0.143 ± 0.020 −0.182 to −0.103 <0.0001 −26% (67–81%)	−0.057 ± 0.013 −0.084 to −0.031 <0.0001 −10% (85–94%)	−0.077 ± 0.025 −0.127 to −0.028 0.003 −19% (69–93%)
Eff. on OBL at given BL	mean ± s.e. c.i. 95% P (2-tailed) % mean (c.i.)	25.64 ± 3.70 12.29 to 32.99 <0.0001 42% (120–154%)	24.53 ± 4.05 16.56 to 32.50 <0.0001 40% (127–153%)	−2.63 ± 2.63 −7.80 to +2.54 0.32 (n.s.) −4% (83–104%)	−5.17 ± 4.13 −13.48 to +3.14 0.22 (n.s.) −6% (84–104%)
Eff. on OBL at given EL	mean ± s.e. c.i. 95% P (2-tailed) % mean (c.i.)	29.81 ± 3.55 22.76 to 36.86 <0.0001 49% (137–160%)	32.98 ± 4.00 25.11 to 40.85 <0.0001 54% (141–166%)	1.67 ± 2.57 −3.31 to +6.82 0.50 (n.s.) 3% (95–111%)	2.97 ± 3.88 −4.83 to +10.78 0.45 (n.s.) 4% (94–113%)

For abbreviations, see Section 2.4. Individual data in Table S1.

3.2. Eye structure in Stygiomysida

3.2.1. Eye Rudiments in *Spelaeomysis bottazzii*

The eye rudiments of postnauplioid to adult stages showed an internal toroidal structure (weakly contrasting in ethanol-fixed material, Figure 7C) with the central pore reaching the dorsal cuticle surface. Toroid diameter 0.08–0.13 mm and 0.8–0.9% BL in adult females with BL 9.1–10.6 mm (n = 7). This structure is identified as an SPO (‘*spo*’ in

Figure 7C). A well-developed OB (‘*ob*’ in Figure 7D) was found at the base of each eyestalk. The OBs contained numerous sensory cells with a neck (small arrow in Figure 7D). Such cells were also found in the OBs of the above troglobiont Mysida species *T. vjetrenicensis* (‘*sc*’ in Figure 1D). SPO and OB are here first described for the order Stygiomysida.

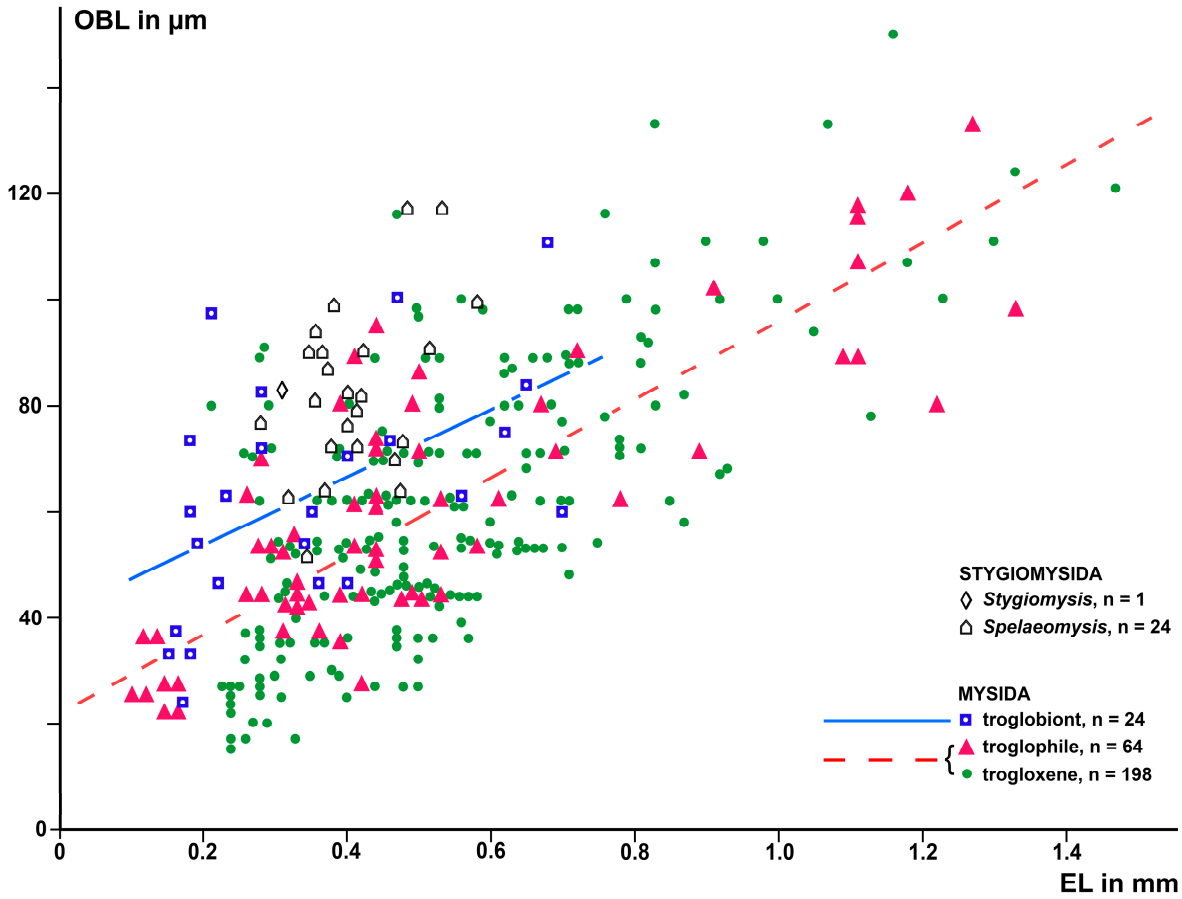

Figure 6. Length of the OB as a response variable versus EL as a predictor variable in separate linear regressions for troglobiont versus combined troglophile and trogloxene mysids (286 specimens of 68 species); data for stygiomysids give no significant regression. Coinciding points are slightly displaced.

The eye rudiments were still in the antero-ventral position at the nauplioid substages N2 and N3. Additional details were not established due to large amounts of oil globules (yolk) visible as granulose structures all along the body in Figure 8A, obstructing the diascopic light path. With the consumption and integration of the dorsal yolk mass and the molt to the postnauplioid stage, the eyes shifted anteriorly and gained a slightly flattened spheroid shape (Figure 8B); SPOs and OBs clearly present, although without staining, weakly contrasting in color from the pale unpigmented eyes (Figure 8C). The freshly hatched juveniles (Figure 8D) showed large, mesially flattened ovoid eyes with some differentiation between the eyestalk and distal rudimentary cornea (Figure 8E); eyestalks with OBs at basis (‘*ob*’ in Figure 8E) and large SPO on the dorsal face (‘*spo*’ in Figure 8E), no rudiments of the ommatidia detected. The eye rudiments were strongly modified during subsequent molt stages, being transformed up to the adult stage into bolsters in the lateral view (Figure 7A) and to broad unpigmented quadrangles without clear differentiation in the eyestalk and cornea in the dorsal view (Figure 7B).

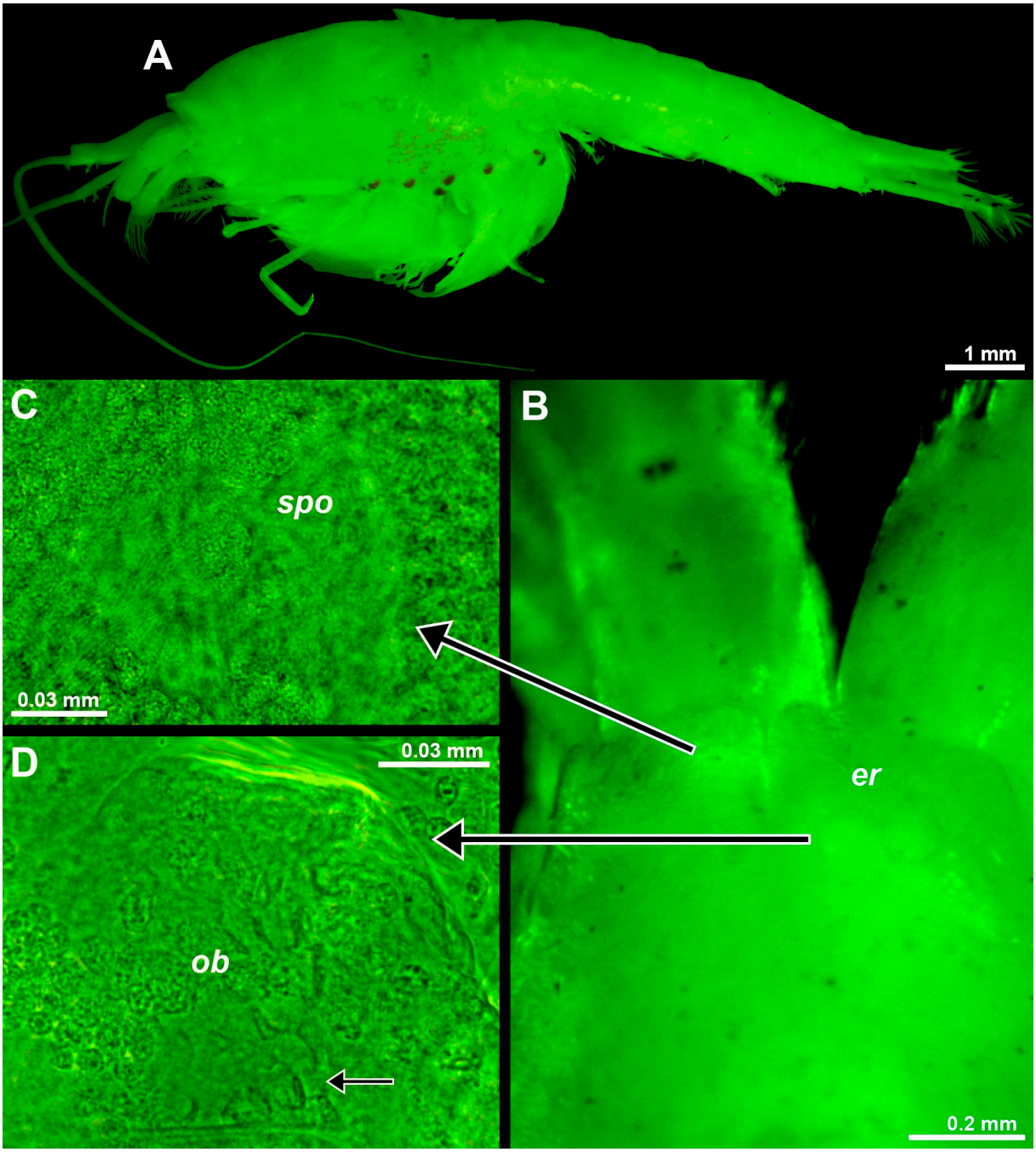

Figure 7. Position and structure of eye rudiments in adult *Spelaeomysis bottazzii*. (**A**) Habitus of adult females with nauplioid larvae, lateral (pigment spots are on the thoracomeres of the female, not on the nauplioids). (**B**) Head of another adult female, dorsal, focus on eye rudiments (*er*), anterior margin of the carapace out of focus. (**C**) Detail of panel (**B**) showing SPO (*spo*), dorsal. (**D**) Detail of panel (**B**) showing OB (*ob*), dorsal, small arrow points to sensory cells with a neck. A, object artificially separated from the background. The green coloring of objects is artificial.

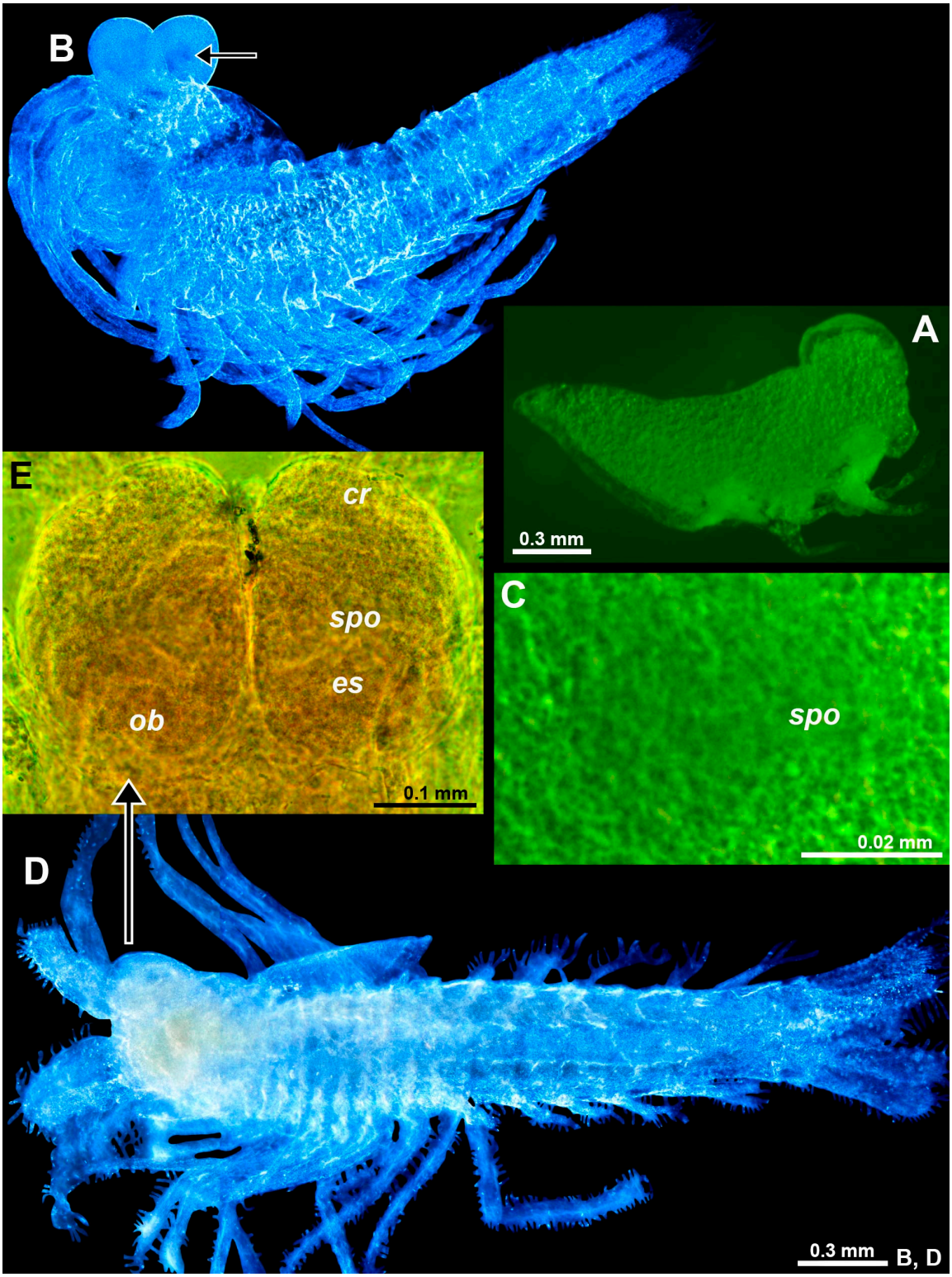

Figure 8. Eye rudiments in the larval and neonate *Spelaeomysis bottazzii*. (**A**) Nauplioid larva, lateral. (**B**) Postnauplioid larva, obliquely dorsal, arrow points to SPO. (**C**) Detail of panel (**B**) showing SPO, dorsal. (**D**) Neonate, ventral. (**E**) Eyes of another neonate, dorsal. Lowercase labels indicate corneal rudiment (*cr*), eyestalk (*es*), OB (*ob*), and SPO (*spo*). The green and blue coloring of objects is artificial. (**B**,**D**), objects artificially separated from the background.

The OBL, EL, and BL measurements were significantly positively correlated with each other and also yielded significant regression lines for the free-living stages (Figure 9). The BL

of adults (n = 24) was 9.80 s.d. ± 1.10 mm, EL 0.410 ± 0.072 mm, and OBL 81.58 ± 15.79 µm. The respective data for postnauplioid larvae (n = 12) were 1.99 ± 0.26 mm, 0.259 ± 0.027 mm, and 74.92 ± 13.93 µm. Surprisingly, the OBLs of postnauplioids (Figure 9B) were not significantly different from those of adults (34 d.f., t = 1.2, p = 0.22). Only measurements of the BL were successful in N2-larvae: mean ± s.d. of BL = 1.70 ± 0.08 mm (n = 21).

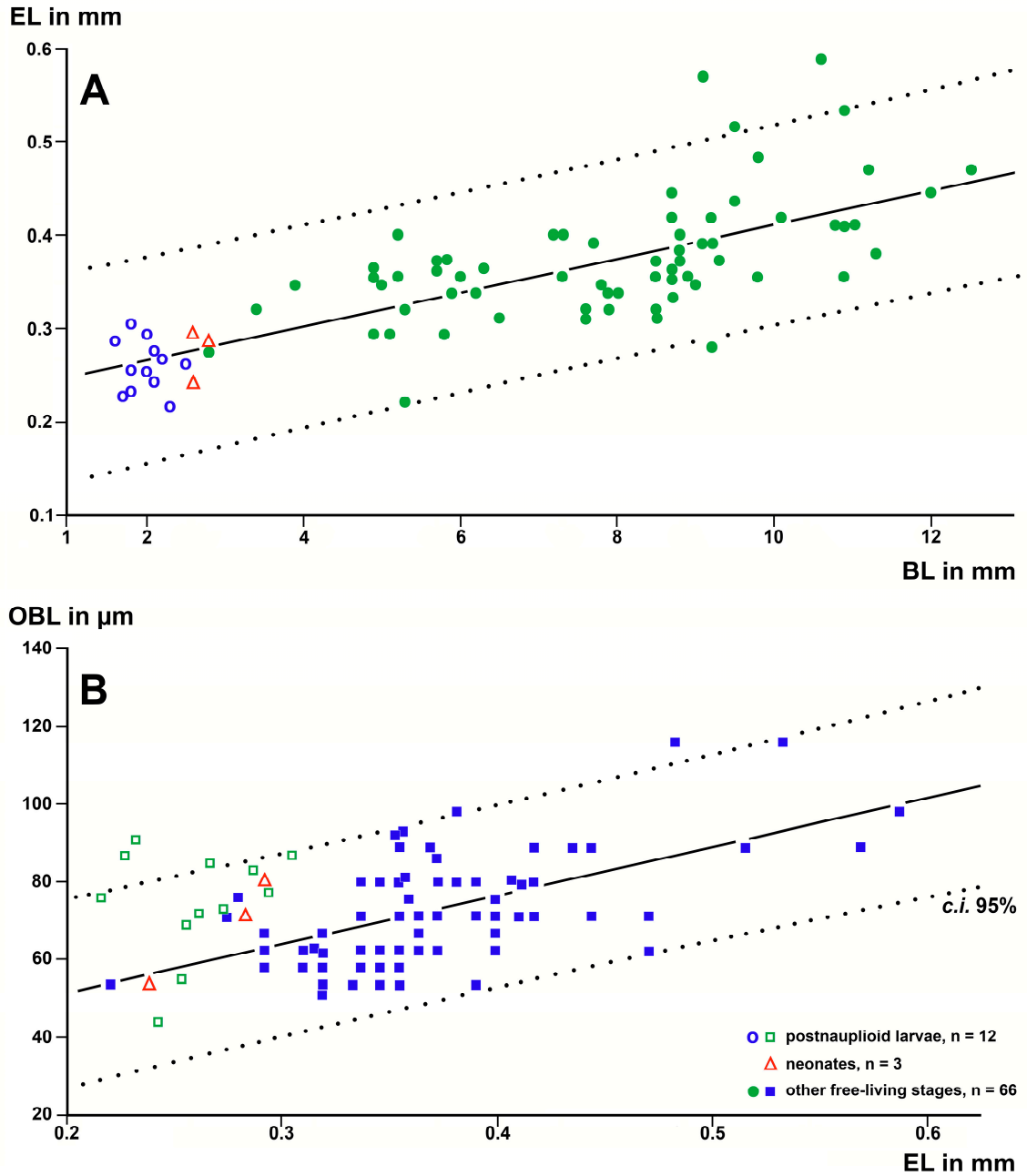

Figure 9. Linear regression analysis of OBL, EL, and BL in postnauplioid larvae and free-living specimens of the troglobiont stygiomysid *Spelaeomysis bottazzii*. (**A**) EL as a response variable, and BL as a predictor variable. (**B**) OBL as a response variable and EL as a predictor variable. Regressions calculated with data from free-living specimens only; data points for postnauplioid larvae added post hoc. Coinciding points are slightly displaced.

3.2.2. Eye Rudiments in *Stygiomysis major*

Only one specimen, a subadult female with BL 15.7 mm (Figure 10A) from the type locality, Jackson's Bay Cave, was available for study; this specimen was not dissected. The

eye rudiments were separate, widening laterally (Figure 10B), shorter than wide, laterally fully extending to the base of the antenna (Figure 10C), mesially only marginally covered by the very short, wide-angled triangular rostrum. A longitudinal groove, labeled '*lg*' in Figure 10B, with some reservation interpreted as separating a mesial eyestalk from a lateral rudiment of the cornea, no rudiments of ommatidia were detected. SPO represented by a toroid (*'spo'* in Figure 10B) around a shallow central depression with the pore reaching to the dorsal surface as described above for *Spelaeomysis bottazzii*. Toroid diameter 0.12 mm or 0.8% BL, respectively, which is also within the range in adult *S. bottazzii*. OB is present, though out of focus, in Figure 10B.

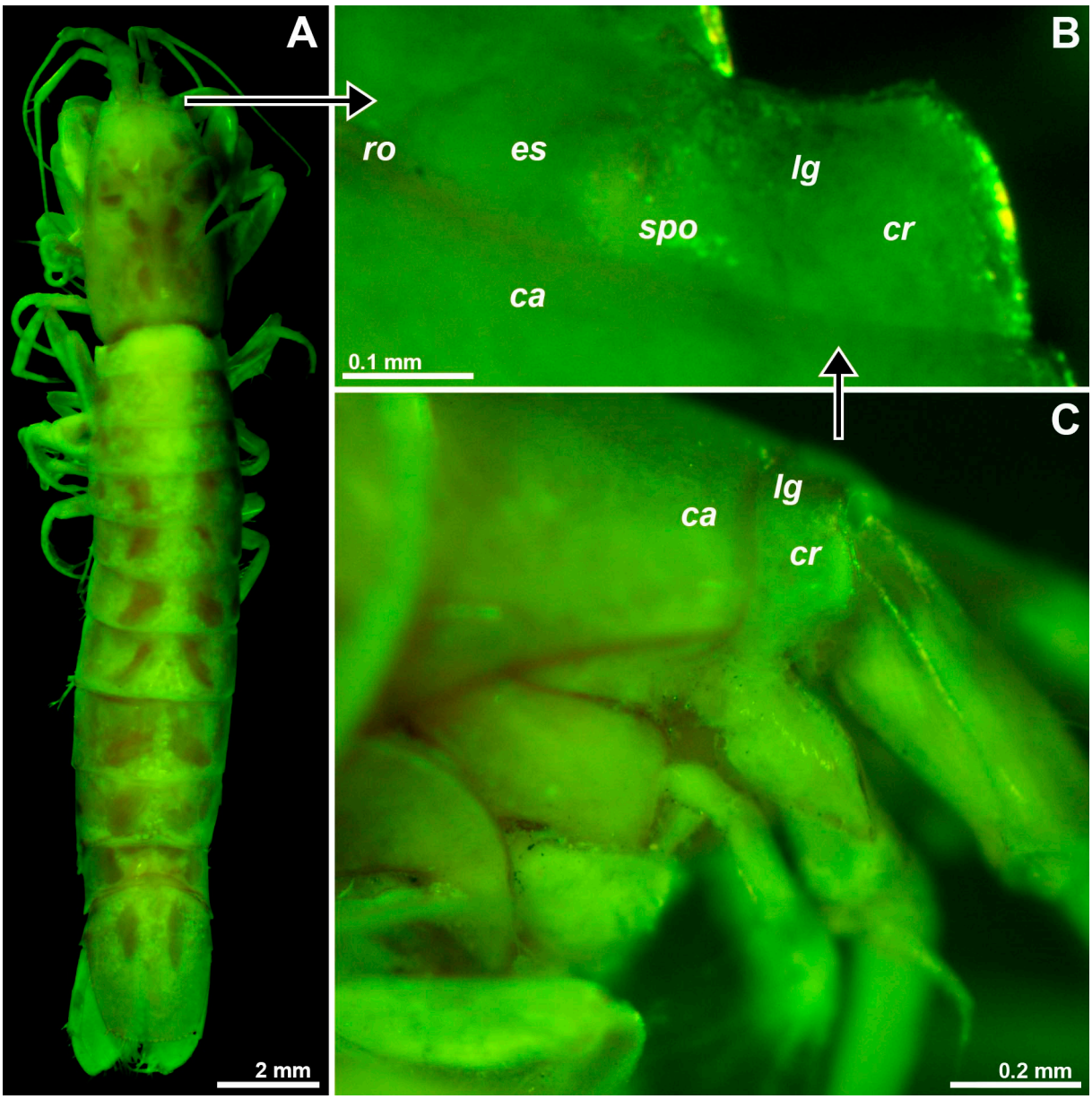

Figure 10. Position and structure of the right eye rudiment in *Stygiomysis major*. (**A**) Habitus of subadult female, dorsal. (**B**) Right eye rudiment, dorsal. (**C**) The cephalic region, lateral. Lowercase labels indicate carapace (*ca*), corneal rudiment (*cr*), eyestalk (*es*), longitudinal groove (*lg*), SPO (*spo*) and rostrum (*ro*). (**A**) object artificially separated from the background. (**A**–**C**), green coloring of objects artificial.

3.2.3. Length of the Organ of Bellonci in Stygiomysida versus Troglobiont Mysida

Differences in OBL between these orders at a given EL and in separate computations at a given BL in 24 + 1 specimens were estimated as explained in Section 2. EL at a given BL of the two stygiomysid species was, on average, 19% shorter than in the five troglobiont mysid species examined (Table 1, Figure 5). By contrast, OB length (Figure 6) did not significantly differ between the troglobionts of the two crustacean orders.

4. Discussion

Stammer [23] (p. 91) was the first to study the internal structure of the eye rudiments in *T. vjetrenicensis*. Subapically, he noted a lamella separating a short, nearly transverse portion from the main body of the eyestalk. From inside this portion, he reported fibers and large nuclei of hypodermal cells. With some reservation, he identified the separate portion of the eye as the former cornea with some nuclei but did not identify rudimentary ommatidia. As discussed below, he erroneously claimed more proximal structures to represent the main, proximally shifted parts of the cornea. The hunchbacked demarcated distalmost portion of the eye rudiments actually presents the only homolog of the cornea [24]. The sub-spherical to oviform structures in the rugged area are here interpreted as strongly reduced ommatidia (Figure 1C).

Stammer [23] (p. 91) noted a cavity with complex content closely below the cuticle of the mesial margin of the eye rudiments and initially interpreted this as a rudiment of lenses. In the appendix [23] (p. 93), clearly added in press, he discussed and left open whether or not the observed cavity may represent an endocrine structure possibly homologous to the X-Organ previously reported [25] for decapods. In a study on the eye of another mysid species, Mayrat [1] finally acknowledged the interpretation as an X-organ (here termed 'Organ of Bellonci') by attributing a typical aspect to the "*pars distalis*" of this organ in *T. vjetrenicensis*. The subunit structuring containing small cavities and sensory cells, as in Figure 1D, fits well with the type of OBs known [2] from many crustacean groups.

A neurosecretory function involved in controlling molting and reproduction was attributed to the OB of a mysid species [21]. Evidence for a non-photoreceptive role was claimed for the OB of another decapod [10]. Nonetheless, other authors [2] assumed a chemosensory or photosensitive function as being most probable. Evidence was also provided that the crustacean hyperglycemic hormone is synthesized in the X-organ/sinus gland complex of the eyestalk, a hormone involved in the osmoregulation of a freshwater decapod [26]. This complex, therefore, appears as the major endocrine control center in most stalk-eyed crustaceans [9]. Finally, the expression of genes coding for neuropeptides was demonstrated in the eyestalk organs of a decapod species [7]. Thus far, however, there is no evidence in favor or against multiple functions.

Whatever else that organ may contribute, photosensitivity appears ecologically plausible in subterranean mysids [6,22]: the anophthalmic hypogean *S. bottazzii* (order Stygiomysida) and the eye-bearing semihypogean *D. camassai* (order Mysida), co-occurring in brackish dolinas, exhibit micro-phytophagy in or near the margins of the photic zone during part of their life cycle. Both species have mandibles capable of scratching epigrowth from hard substrates. A preceding replenishment of trophic reserves could be important prior to entering deep, nutrient-poor groundwater where the incubating females of the hypogean *Spelaeomysis* may escape from predation by epigean animals. Only 'fat' specimens produce eggs [6]. Nonetheless, females incubating eggs are, on average, fatter than those with larvae, which points to unfavorable nutritional conditions during the very long incubation, which ends with the release of the young and a molt to a post-reproductive stage with reduced oostegites. This makes it plausible that the females could profit from detailed sensory feedback when transitioning between risky photic and nearby, safer aphotic habitats. The contribution of potential photic, olfactory, and 'auditory' sensitivity to this feedback remains a challenging question.

Based on a sample of 68 Mysida species, Table 1 and Figures 5 and 6 show that adult EL at a given BL is, on average, 26% (c.i. 95% based on specimen numbers: 19–33%) shorter

in troglobiont versus trogloxene species, while the OB is 54% longer (41–66%) at a given EL and 40% (27–53%) longer at given BL, respectively, in troglobiont species. These findings clearly demonstrate that the OB proliferates, whereas the eyes are reduced in troglobiont species. This points to several potential sensory functions (possibly in addition to other functions) of the OB in Mysida. The structure of antennal sensilla in a subterranean mysid species suggests that the loss of visual abilities could be counterbalanced by more effective tactile and chemosensory abilities [27]. In that respect, the role of OBs remains pending and calls for additional physiological data from anophthalmic mysids before drawing further conclusions.

Using standard microscopy, no OBs were found in nauplioid larvae (the first larval stage in the marsupium of Mysida and Stygiomysida). The OBs became well visible at the subsequent postnauplioid stage in the marsupium. The first appearance of OBs varies in the range of larval stages I to V among species of decapods [28]. The here-presented first finding for mysidacean larvae may be related to the incomplete eyes (Figure 3A–D) of the almost immotile nauplioid larvae versus well-formed eyes (Figures 3F and 8B) in postnauplioids, which are capable of small movements in the marsupium.

In the troglobiont *S. bottazzii*, the postnauplioid larvae still show almost spherical eyes (Figure 8B) with pale cornea, whereas neonates feature large eyes (Figure 8D,E) shaped as flattened ovoids with some differentiation in eyestalk and rudimentary cornea [6]. During subsequent molt stages, the eyes once again become more flattened and take on a quadrangular shape without clear differentiation into eyestalk and cornea. The eye rudiments remain separate up to the adult stage. This species shows a clear regressive ontogenetic eye development. Similarly, a strong ontogenetic regression occurs in *S. longipes* (Pillai & Mariamma, 1964), whose paired conical eyes show no trace of ommatidia in postnauplioids, the eye rudiments then fusing mesially to form a single eyeplate in the adult [29]. Optical ganglia inside eyeplates have been reported for this species from freshwater wells in India, but neither OBs nor SPOs [29]. If the large eyes of early stages (Figure 8D,E) in *S. bottazzii* have any sensorial functions, they may be related to life in near-surface habitats, whereby adult females are rare near the surface, probably mainly incubating in deep brackish groundwater [5,6].

Although a total of eight genus names were proposed in the past in the order Stygiomysida, only two genera, *Spelaeomysis* with nine species, and *Stygiomysis* Caroli, 1937, with seven species, are currently acknowledged. Toroidal structures with a central pore dorsally on the eyestalks (Figure 10B), interpreted as SPOs, were detected here for the first time for this order, namely in one species for each of the genera, representing separate families (Stygiomysidae and Lepidomysidae). In an analogy, toroids with a central pore were found at the tip of the sensory papilla on the eyestalks in the mysid *M. gibbosa* (Figure 2E,F). In most mysids, however, the sensory pores are not on papillae but associated with the OB (Figures 1E and 3C,D). Sensory pores with putative chemoreceptive function on eyestalk papillae are also present in certain decapods [2]. A chemosensory function also appears plausible for the pores on the eyestalks of Mysida and Stygiomysida, but experimental and ultrastructural data are still needed.

Supplementary Materials: The following supporting information can be downloaded at: https://www.mdpi.com/article/10.3390/arthropoda1040019/s1, Table S1: Sampling data, troglophilia, and measurements related to body length, eye length, and length of the Organ of Bellonci in Mysida and Stygiomysida.

Funding: This research received no external funding.

Institutional Review Board Statement: Not applicable; only long-term preserved materials studied.

Informed Consent Statement: Not applicable.

Data Availability Statement: See Supplementary Materials.

Acknowledgments: The author is greatly indebted to Daniel Abed-Navandi (Vienna), Gerlinde Aichinger (Salzburg), Antonio P. Ariani (Naples), Torleiv Brattegard (Bergen), Pierre Chevaldonné (Marseille), Mikhail Daneliya (Helsinki), Yukio Hanamura (Yokohama), Thomas Huber (Vienna), Thomas M. Iliffe (Galveston), Wulf C. Kobusch (Bochum), Masaaki Murano (Tokyo), W. Wayne Price (Tampa), Klaus Rudolph (Brandenburg an der Havel), Armin Svoboda (Bochum), and Peter Wirtz (Faro) for providing materials for examination.

Conflicts of Interest: The author declares no conflict of interest.

References

1. Mayrat, A. Oeil, centres optiques et glandes endocrines de *Praunus flexuosus* (O.F. Müller). *Arch. Zool. Exp. Gén.* **1956**, *93*, 319–366.
2. Hallberg, E.; Chaigneau, J. The non-visual sense organs. In *The Crustacea. Revised and Updated from the Traité de Zoologie*; Forest, J., von Vaupel Klein, J.C., Eds.; Brill: Leiden, The Netherlands, 2004; Volume 1, pp. 301–380.
3. Bellon-Humbert, C. *Développement Embryonnaire de Palaemon serratus, Résultats Préliminares*; IFREMER: Montpellier, France, 1983; pp. 181–194.
4. Melville, R.; Smith, J.D.D. *Official Lists and Indexes of Names and Works in Zoology*; International Trust for Zoological Nomenclature: London, UK, 1987; pp. 1–366.
5. Ariani, A.P.; Wittmann, K.J. The transition from an epigean to a hypogean mode of life: Morphological and bionomical characteristics of *Diamysis camassai* sp. nov. (Mysidacea, Mysidae) from brackish-water dolinas in Apulia, SE-Italy. *Crustaceana* **2002**, *74*, 1241–1265. [CrossRef]
6. Ariani, A.P.; Wittmann, K.J. Feeding, reproduction, and development of the subterranean peracarid shrimp *Spelaeomysis bottazzii* (Lepidomysidae) from a brackish well in Apulia (southeastern Italy). *J. Crust. Biol.* **2010**, *30*, 384–392. [CrossRef]
7. Ventura-López, C.; Gómez-Anduro, G.; Arcos, F.G.; Llera-Herrera, R.; Racotta, I.S.; Ibarra, A.M. A novel CHH gene from the Pacific white shrimp *Litopenaeus vannamei* was characterized and found highly expressed in gut and less in eyestalk and other extra-eyestalk tissues. *Gene* **2016**, *582*, 148–160. [CrossRef] [PubMed]
8. Steele, V.J.; Oshel, P.E. Ultrastructure of the attachment cells of the organ of Bellonci in *Gammarus setosus* (Crustacea, Amphipoda). *J. Morphol.* **1989**, *200*, 93–119. [CrossRef] [PubMed]
9. Reddy, P.R.; Reddy, P.S. *Eyestalk Hormones on Molting and Reproduction. Concepts of Neuropeptide Hormones in Crab*; Lambert Academic Publishing: Saarbrücken, Germany, 2012; pp. 1–172.
10. Hallberg, E.; Kauri, T. Evidence of non-photoreceptive function of the sensory units of the Organ of Bellonci in *Macrobrachium rosenbergii* (Decapoda, Caridea). *Crustaceana* **1992**, *62*, 137–141. [CrossRef]
11. Wittmann, K.J. Comparative biology and morphology of marsupial development in *Leptomysis* and other Mediterranean Mysidacea (Crustacea). *J. Exp. Mar. Biol. Ecol.* **1981**, *52*, 243–270. [CrossRef]
12. Wittmann, K.J.; Chevaldonné, P. First report of the order Mysida (Crustacea) in Antarctic marine ice caves, with description of a new species of *Pseudomma* and investigations on the taxonomy, morphology and life habits of *Mysidetes* species. *ZooKeys* **2021**, *1079*, 145–227. [CrossRef] [PubMed]
13. Culver, D.C.; Pipan, T. Ecological and evolutionary classification of subterranean organisms. In *Subterranean Biology in the Anthropocene*; Reboleira, A.S.P.S., Mendes Gonçalves, F.J., Eds.; ARPHA Conference Abstracts; Pensoft: Sofia, Bulgaria, 2018; Volume 1, p. e29878. [CrossRef]
14. Pesce, G.L.; Juberthie-Jupeau, L.; Passelaigue, F. *Mysidacea. Encyclopaedia Biospeologica*; Juberthie, C., Decu, V., Eds.; Société Internationale de Biospéologie: Moulis, France, 1994; Volume 1, pp. 113–119.
15. Wittmann, K.J. Untersuchungen zur Lebensweise und Systematik von *Leptomysis truncata* und zwei verwandten Formen (Crustacea, Mysidacea). *Ann. Naturhist. Mus. Wien* **1986**, *87B*, 295–323.
16. Wittmann, K.J.; Chevaldonné, P. Description of *Heteromysis* (*Olivemysis*) *ekamako* sp. nov. (Mysida, Mysidae, Heteromysinae) from a marine cave at Nuku Hiva Island (Marquesas, French Polynesia, Pacific Ocean). *Mar. Biodiv.* **2016**, *47*, 879–886. [CrossRef]
17. Ariani, A.P.; Wittmann, K.J. Alcuni aspetti della biologia della riproduzione in *Spelaeomysis bottazzii* Caroli (Mysidacea, Lepidomysidae). *Thalassia Salentina* **1999**, *23*, 193–200.
18. Weber, E. *Grundriss der Biologischen Statistik*, 6th ed.; Gustav Fischer Verlag: Jena, Germany, 1967; pp. 1–674.
19. XLSTAT. Available online: https://www.xlstat.com (accessed on 17 July 2023).
20. Wittmann, K.J.; Ariani, A.P.; Lagardère, J.-P. Orders Lophogastrida Boas, 1883, Stygiomysida Tchindonova, 1981, and Mysida Boas, 1883 (also known collectively as Mysidacea). In *The Crustacea. Revised and Updated from the Traité de Zoologie*; von Vaupel Klein, J.C., Charmantier-Daures, M., Schram, F.R., Eds.; Brill: Leiden, The Netherlands, 2014; Volume 4.
21. Cuzin-Roudy, J.; Saleuddin, A.S.M. A study of the neurosecretory centres of the eyestalk in *Siriella armata* M. Edw. (Crustacea: Mysidacea). *Can. J. Zool.* **1985**, *63*, 2783–2788. [CrossRef]
22. Ariani, A.P.; Wittmann, K.J. Interbreeding versus morphological and ecological differentiation in Mediterranean *Diamysis* (Crustacea, Mysidacea), with description of four new taxa. *Hydrobiologia* **2000**, *441*, 185–236. [CrossRef]
23. Stammer, H.-J. Ein neuer Höhlenschizopode, *Troglomysis vjetrenicensis* n.g. n.sp. Zugleich eine Übersicht der bisher aus dem Brack- und Süßwasser bekannten Schizopoden, ihrer geographischen Verbreitung und ihrer ökologischen Einteilung—Sowie eine Zusammenstellung der blinden Schizopoden. *Zool. Jb. Syst.* **1936**, *68*, 53–104.

24. Wittmann, K.J.; Ariani, A.P.; Daneliya, M. The Mysidae (Crustacea: Peracarida: Mysida) in fresh and oligohaline waters of the Mediterranean. Taxonomy, biogeography, and bioinvasion. *Zootaxa* **2016**, *4142*, 1–70. [CrossRef] [PubMed]
25. Hanström, B. Über das Organ X, eine inkretorische Gehirndrüse der Crustaceen. *Psychiat. Neurol. Bl. Amst.* **1934**, *38*, 141–154.
26. Serrano, L.; Grousset, E.; Charmantier, G.; Spanings-Pierrot, C. Occurrence of L—And D-Crustacean Hyperglycemic Hormone Isoforms in the Eyestalk X-Organ/Sinus Gland Complex during the ontogeny of the crayfish *Astacus leptodactylus*. *J. Histochem. Cytochem.* **2004**, *52*, 1129–1140. [CrossRef]
27. Crouau, Y. Etude externe de l'équipement sensoriel des antennes 1 et 2 d'un Crustacé Mysidacé souterrain *Antromysis juberthiei* Bacesco et Orghidan. *Arch. Zool. Exp. Gén.* **1981**, *122*, 271–288.
28. Rotllant, G.; Charmantier-Daures, M.; Trilles, J.P.; Charmantier, G. Ontogeny of the sinus gland and of the organ of Bellonci in larvae and postlarvae of the European lobster *Homarus gammarus*. *Inverteb. Repro. Dev.* **1994**, *26*, 13–22. [CrossRef]
29. Nath, C.N.; Thampy, D.M.; Pillai, N.K. Optic regression in a subterranean mysid (Crustacea, Mysidacea). *Int. J. Speleol.* **1972**, *4*, 51–54. [CrossRef]